DEVELOPMENTAL CIGARETTE SMOKE EXPOSURE: KIDNEY PROTEOME PROFILE ALTERATIONS IN LOW BIRTH WEIGHT PUPS

J Rekha[1], **Jing Chen**[2], **Lorena Canales**[2], **Todd Birtles**[1], **M. Michele Pisano**[1,3], and **Rachel E. Neal**[2,3,4]

[1]Department of Molecular, Cellular, and Craniofacial Biology, ULSD, University of Louisville, Louisville, KY

[2]Department of Environmental and Occupational Health Sciences, School of Public Health and Information Sciences, University of Louisville, Louisville, KY

[3]Birth Defects Center, University of Louisville, Louisville, KY

Abstract

The Brenner hypothesis states that a congenital reduction in nephron number predisposes to adult-onset hypertension and renal failure. The reduction in nephron number induced by proportionally smaller kidney mass may predispose offspring to glomerular hyperfiltration with maturity onset obesity. Developmental cigarette smoke exposure (CSE) results in intrauterine growth retardation with a predisposition to obesity and cardiovascular disease at maturity. Utilizing a mouse model of 'active' developmental CSE (gestational day [GD] 1-postnatal day [PD] 21; cotinine>50 ng/mL) characterized by persistently smaller offspring with proportionally decreased kidney mass, the present study examined the impact of developmental CSE on the abundance of proteins associated with cellular metabolism in the kidney. Following cessation of CSE on PD21, kidney tissue was collected from CSE and Sham exposed pups for 2D-SDS-PAGE based proteome profiling with statistical analysis by Partial Least Squares-Discriminant Analysis (PLS-DA) with affected molecular pathways identified by Ingenuity Pathway Analysis. Proteins whose expression in the kidney were affected by developmental CSE belonged to the inflammatory disease, cell to cell signaling/interaction, lipid metabolism, small molecule biochemistry, cell cycle, respiratory disease, nucleic acid and carbohydrate metabolism networks. The present findings indicate that developmental CSE alters the kidney proteome. The companion paper details the liver proteome alterations in the same offspring.

Keywords

developmental cigarette smoke exposure; CSE; proteome; kidney

[4]Corresponding Author: rachel.neal@louisville.edu; 485 E. Gray Street, Louisville, KY 40292.

1. INTRODUCTION

Approximately 20% of women smoke throughout pregnancy (Centers for Disease Control and Prevention, 2001). Non-facilitated transfer of small molecular weight and highly water soluble components of cigarette smoke across the placenta results in exposure of the fetus to the toxic compounds contained in cigarette smoke. Cigarette smoke is a heterogenous mixture of chemical compounds including nicotine, acetone, acrolein, carbon monoxide, toxic metals (lead, arsenic, cadmium, mercury), and polycyclic aromatic hydrocarbons such as benzo(a)pyrene (Rahman and Mac Nee, 1996; Sisman *et al.*, 2003; Kyerematen and Vesell, 1991; Shah and Helfant, 1988; Zavos, 1989; Stack and Murthy, 2010). In epidemiological studies, developmental cigarette smoke exposure is associated with numerous adverse fetal outcomes including *in utero* growth restriction, low birth weight, and stillbirth (March of Dimes, 2010; Centers for Disease Control and Prevention. 2010). In rodent models, a similar host of developmental abnormalities following prenatal cigarette smoke exposure (CSE) are observed including low birth weight and functional impairments such as delayed cognitive development (Zdravkovic *et al.*, 2005; Boadi *et al.*, 1992; Shea and Steiner, 2008; Tomatis, 1989; Esposito *et al.*, 2008).

Low birth weight is a risk factor for multiple maturity onset diseases including diabetes, hypertension, and cardiovascular disease (March of Dimes, 2010). Low birth weight and nephron number are linked through proportional reductions in kidney mass (Hughson *et al.*, 2003). Both are positively associated with the development of hypertension (Abitbol and Ingelfinger, 2009). The putative link between developmental CSE and adult onset hypertension and/or cardiovascular disease may be attributed in part to mild structural dysmorphology and proportionally smaller kidney size (Czekaj *et al.*, 2002; Nelson *et al.*, 1999). *In utero* passive CSE at defined developmental windows (pre-, during, and post-organogenesis) induced growth retardation paired with increased kidney cellular apoptosis, delayed glomerular maturation, and mesenchymal histological abnormalities (Nelson *et al.*, 1999). It remains unknown whether kidney metabolic activity contributes to the development of hypertension and chronic kidney disease in adulthood. The present study examined the impact of developmental CSE on the kidney proteome - specifically on the expression of metabolic proteins - in a mouse model of "active" CSE that results in reduced animal weight with attendant decreases in organ mass including that of the kidney.

2. MATERIALS AND METHODS

2.1 Animals

Adult C57BL/6J mice were purchased from The Jackson Laboratory (Bar Harbor, ME). Animals were housed by the University of Louisville in a dedicated room at 22°C, with a 12 hour alternating light/dark cycle, and were maintained on Purina LabDiet #5015 and water *ad libitum*. Timed pregnancies were obtained by overnight mating of a single mature male with two nulliparous females (plug positive designated GD0).

2.2 Cigarette Smoke Exposure Model

On GD0, mouse dams were randomly assigned to either the Sham exposure (n=9) or cigarette smoke exposure (CSE; n=9) group. Dams (and subsequent litters) were exposed to ambient air (sham-exposed controls) or cigarette smoke for 6 hours per day, seven days per week, from GD0 through PD21 as per the companion article (Canales *et al.*, 2012).

On PD21, Sham exposed and CSE animals were euthanized by CO_2 asphyxiation followed by cervical dislocation. Kidneys were dissected and immediately stored at −80°C until analysis. Kidney wet weights from the offspring utilized in this study as well as additional experimental animals were determined for a total of 18 Sham exposed and 12 CSE kidneys.

A single kidney each from two pups per litter was weighed (n=9 Sham litters and 6 CSE litters). The remaining pups from each litter were followed until adulthood with assessment of cognitive function and other measures of neurodevelopment (subject of future manuscript).

2.3 Proteomics Analysis

Detailed experimental procedures are given in the companion paper relating the impact of developmental CSE on liver proteome profiles (Canales *et al.*, 2012). In brief, kidney tissue was homogenized in 7M urea, 2M thiourea, and 40mM dithiothreitol (DTT). 400 μg of protein (Bradford assay; Bradford 1976) was separated by isoelectric focusing followed by SDS-PAGE with Coomassie Blue dye for visualization of protein spots and densitometric analysis performed with Progenesis SameSpots software (Nonlinear Dynamics; New Castle-on-Tyne, UK). Protein spots of interest were identified by LTQ-MS/MS with collision induced dissociation and MASCOT searching of the NCBInr database. A total MOWSE protein probability score greater than 100 was considered acceptable (Neuhoff *et al.*, 1985).

Partial Least Squares-Discriminant Analysis (PASW Statistics 18) was used to describe the separation of the Sham exposed and CSE groups (Karp *et al.*, 2005). Variable Importance in Projection (VIP) score ranking of proteins spot abundances was utilized to identify putative proteins of interest with an empirically determined cutoff point (Karp *et al.*, 2005). Ingenuity Pathway Analysis was used to determine metabolic pathways related to proteins in the kidney whose levels were altered by developmental CSE and that were identified by PLS-DA as features describing the differences between groups (Ingenuity Systems, 2010).

3. RESULTS

3.1. Exposure Conditions and Neonatal Outcomes

The sham/cigarette smoke inhalation exposure chamber conditions and the developmental outcomes of the Sham exposed and CSE groups are identical to those in the companion paper examining the impact of developmental CSE on liver proteome profiles (Canales *et al.,* 2012) and similar to the outcomes of our prior report establishing this model (Esposito *et al.,* 2008). The model system employed for the current study is an "active" exposure paradigm with serum cotinine levels in the dams and pups greater than 50 ng/mL. This model exhibits a decrease in birth weight that persists through cessation of exposure at weaning on PD21 (13.2% decrease in weight of CSE offspring). Dam weights, number of pups, viability, and sex ratio were not impacted by CSE. At parturition, litters were maintained without culling or fostering.

As shown in Figure 1, offspring kidney wet weights were decreased in the CSE versus the Sham exposed groups at PD21 (p<0.01) by ~15%, similar to our previously published decrements in fetal body and brain weights in this mouse model (Esposito *et al.*, 2008). The ratio of offspring kidney wet weight per total body weight was not impacted by developmental cigarette smoke exposure. A single kidney sample per litter from representative litters (9 Sham and 9 CSE) was utilized for proteome profiling.

3.2. Kidney Proteome Profiles

Representative 2D-SDS-PAGE gels of kidney proteins from Sham exposed and CSE offspring are shown in Figure 2. The proteins on the gels spanned an isoelectric focusing range of 3 to 10, with the acidic proteins on the left and the basic proteins on the right of the gel image, and with descending molecular weights ranging from ~80 kDa to ~11 kDa. Several protein spots were identified to validate the molecular weight range. The spot

patterns of the kidney proteins from Sham exposed and CSE groups were similar with varying protein spot abundance as the predominant difference between groups.

3.3. Partial Least Squares-Discriminant Analysis

An empirical fold change minimum (e.g.: 2-fold change) was not employed as a cutoff for determination of significance of impact of protein spot density. Rather, a ranked order of importance (Variable Import in Projection: VIP) of protein spot densities was utilized in defining the differences between groups after building a multivariate inverse least squares discriminant model to classify sample groupings. Noise, identified by a sharp increase in slope of 3-D plot of spot pixel density or an aggregate normalized pixel depth of less than 1000, was removed from the dataset prior to PLS-DA modeling. Sequential PLS-DA models were generated with the stepwise exclusion of the bottom twenty VIP ranked protein spots until a gradual loss of separation of the groups was evident in a three dimensional plot of the top 3 latent factors. Approximately 45 protein spots (VIP 1.5) were found to contribute to the separation in kidney proteome profiles between the Sham exposed and CSE groups. As shown in Figure 3A, when abundances of all proteins were included (noise excluded), the first latent factor accounted for 58% of the variance between the Sham exposed and CSE groups and the second latent factor accounted for an additional 32% of the variance. As shown in Figure 3B, the proteome profiles of the Sham exposed and CSE groups are distinct. The separation between the groups is depicted by graphing latent factors 1, 2 and 3.

3.4. Proteins impacted by CSE

In Figure 4, a representative 2D-SDS-PAGE kidney protein spot map is shown with color coded numbers labeling the top 45 protein spots (based on VIP 1, 2, or 3 rankings) describing the differences between the Sham exposed and CSE kidney proteome profiles as determined by Partial Least Squares-Discriminant Analysis. The proteins with decreased abundance are labeled with a blue number, while the proteins with increased abundance are shown by a green number. The proteins (*decreased* and *increased* abundance) contributing to the separation of groups according to the PLS-DA model are listed in Table 1. For several spots, more than one protein was identified indicating that a mixture of proteins with similar isoelectric focusing point and molecular weight are present within the spot.

3.5. Ingenuity Pathway Analysis

Proteins identified in spots contributing to the separation between the groups were categorized as increased or decreased in abundance in the kidney of the CSE group and imported for IPA analysis. Proteins that represent the predominant contribution to the spot intensity, as determined by a minimum of 200% of the MOWSE score of the next ranked protein identified, were included in the identification of nodes of interest within the affected networks (see Table 1). The analysis did not include proteins from **Spot 4** (and similar **Spots 3, 6, 13, 14, 16, 20, 21, 23, 24, 27, 35, 37, 39, 40**) since the relative MOWSE scores for identification of the multiple proteins within the spot were similar and therefore a single likely candidate for alteration in abundance could not be identified. In **Spot 1**, this is not the case. Aldo-keto reductase family 1, member A4 is clearly the dominant protein in the spot (MOWSE score 671) while D-amino acid oxidase is present in much lower abundance (MOWSE score 138). In this case, Aldo-keto reductase family 1, member A4 was included in the IPA analysis.

In the associated figures, solid lines indicate a direct interaction while dotted lines indicate an indirect interaction. Geometric shapes identify classes of proteins: cytokines (square), growth factors (dotted square), phosphatases (triangle), kinases (inverted triangle), ligand-dependent nuclear receptors (rectangle), G-protein coupled receptors (vertical rectangle), ion channels (dotted vertical rectangle), peptidases (horizontal diamond), enzymes (vertical

diamond), transcription regulators (horizontal ellipse), transmembrane receptors (vertical ellipse), transporters (trapezoid), and other important molecules (circle).

3.5.1. Proteins With Decreased Abundance in the Kidney of CSE Mice—

Dominant or single proteins with decreased abundance in kidneys of CSE mice were grouped by membership in metabolic networks via IPA analysis. Proteins in **Spots 1, 2, 7, 9, 18** consisting respectively of: Aldoketoreductase family 1, member A4; Aldoketoreductase family 1, member B1; Acetyl-coenzyme A acetyltransferase 1 precursor; Mitochondrial short-chain enoyl-coenzyme A hydratase 1; and Calbindin-28K are members of the *lipid metabolism network*. Proteins in **Spots 1, 2, 7, 9, 11, 13, 14, 15, 17, 18, 19, 22, 24** consisting respectively of: Aldoketoreductase family 1, member A4; Aldoketoreductase family 1, member B1; Acetyl-coenzyme A acetyltransferase 1 precursor; Mitochondrial short-chain enoyl-coenzyme A hydratase 1; Peroxiredoxin 1; Aldolase B; Malate dehydrogenase 2; Mitochondrial ATP synthase beta subunit; Calreticulin; Calbindin-28K; Transferrin; Glycerol-3-phosphate dehydrogenase; and Carbonic anhydrase II are members of the *small molecule biochemistry network*.

Figure 5 depicts a portion of the *lipid metabolism and small molecule biochemistry networks*. Proteins with *decreased* abundance in the CSE group are shaded in gray. A central node in the network is Solute Carrier Family 2 (Facilitated Glucose Transporter Member 4). The following protein spots were linked to this node: **Spot 7** (Acetyl-CoA acyltransferase 2), **Spot 9** (Mitochondrial short-chain enoyl-coenzyme A hydratase 1), **Spot 13** (Aldolase B). Spots with multiple proteins of equivalent abundance also support the designation of alteration in this pathway, although the designation of a decrease in pixel density of these spots cannot be unambiguously attributed to the specific network member protein. The following proteins are part of this network however more than one protein was present in the spots: **Spot 3** (Voltage-dependent anion channel 2, Electron transfer flavoprotein alpha polypeptide); **Spot 6** (Enolase 1); **Spot 21** (Aldehyde dehydrogenase 6 family, member A1). Homogentisate 1, 2-dioxygenase (**Spot 6**) is listed in the network but not shown in the figure. For **Spot 3**, both proteins identified as present in the spot belong to this node. Similarly for **Spot 6**, two of the three proteins present were related to this node. Seven proteins present in **Spots 3, 6, 7, 9** and **13** were considered supportive of the designation of a probable alteration in the SCF2 node of the lipid metabolism and small molecule biochemistry networks in kidney of CSE offspring. Though other nodes exist in this network, limited individual protein spot identifiers were linked to these nodes.

Three additional networks contained proteins with decreased abundance in the kidney of CSE mice. The following proteins in **Spots 2, 6, 12, 13, 15, 21, 22** of the *nucleic acid metabolism network* were decreased: Aldoketoreductase family 1, member B1; Homogentisate 1,2-dioxygenase; Glyceraldehyde-3-phosphate dehydrogenase; Aldolase B; Mitochondrial ATP synthase beta subunit; 3-oxoacid CoA transferase 1; and Glycerol-3-phosphate dehydrogenase. For the *respiratory disease network*, proteins in **Spots 11, 12, 19, and 24** consisting of: Peroxiredoxin 1; Glyceraldehyde-3-phosphate dehydrogenase; Transferrin; and Carbonic Anhydrase were decreased in abundance in the kidney following developmental CSE. The *inflammatory disease network* possessed the following proteins with decreased abundance from **Spots 1, 11, 12, 13, 17, 19, 24**: Aldoketo reductase family 1, member A1; Peroxiredoxin 1; Glyceraldehyde-3-phosphate dehydrogenase; Aldolase B; Calreticulin; Transferrin; and Carbonic Anhydrase.

Figure 6 shows a portion of the *inflammatory disease, respiratory disease and nucleic acid metabolism networks*. The proteins identified in this network had *decreased* abundance in the kidney of the CSE group. Nuclear receptor subfamily 3 group C member 1 (NR3C1; glucocorticoid receptor) is a chief node in the network. The following protein spots were

associated with the NR3C1 node: **Spot 11** (Peroxiredoxin 1 as dominant protein); **Spot 12** (Glyceraldehyde-3-phosphate dehydrogenase); **Spot 17** (Calreticulin); and **Spot 19** (Transferrin as dominant protein, Albumin as minor protein). Homogentisate 1, 2-dioxygenase (**Spot 6**) is linked to this node through Glyceraldehyde-3-phosphate dehydrogenase (**Spot 12**) but cannot be counted as support for the designation of an alteration in this node due to the presence of multiple proteins in **Spot 12**. The presence of five proteins including 3 single proteins per spot and a dominant and minor protein in a spot from **Spots 11, 12, 17,** and **19** indicate that the NR3C1 network node may be affected in the kidney by developmental CSE.

Insulin, another central node in the *inflammatory disease, respiratory disease and nucleic acid metabolism networks*, is impacted in the kidney of CSE offspring. The following proteins were connected to the Insulin node: **Spot 7** (Acetyl Co-A acetyltransferase 1); **Spot 15** (ATP synthase, H$^+$ transporting, mitochondrial F1); and **Spot 18** (Calbindin 1, 28 kDa). Proteins from **Spots 4, 14, and 19** were altered in support of the inference of an alteration in this node. However, each spot possesses multiple proteins and therefore unambiguous attribution of alterations in abundance to a single protein cannot be made. The contribution of Phosphoglycerate kinase 1 (**Spot 4**), Malate dehydrogenase 2, NAD mitochondrial (**Spot 14**), and Albumin (minor component of **Spot 19**) must be judged as unsubstantiated. Identification of this node as affected in the kidney by developmental CSE is primarily supported by a decreased in abundance of 3 proteins from 3 separate spots.

In summary, 15 proteins in the kidney that decreased in abundance with developmental CSE (either a single or dominant protein in a spot) were attributed to redundant membership in multiple metabolic networks. These networks possess 3 nodes that may be impacted by developmental CSE: Solute Carrier Protein 2 (GLUT4), Nuclear receptor subfamily 3 group C member 1 (NR3C1), and Insulin.

3.5.2. Proteins With Increased Abundance in the Kidney of CSE Mice—

Dominant or single proteins in spots with increased abundance in kidney following developmental CSE were grouped by membership in metabolic networks via IPA analysis. The *small molecule biochemistry network* possessed four spots with increased pixel density **(Spots 27, 32, 36, 42)** with the following proteins affected: ATPs synthase, H+ transporting, mitochondrial F1 complex, alpha subunit; NADH-ubiquinone oxidoreductase 75 kDa subunit; Tumor metastatic process-associated protein NM23; and Glutathione Peroxidase. The *cell to cell signaling and interaction network* was also impacted with proteins from **Spots 30, 34, 36, 42** possessing increased abundances in the kidney following developmental CSE. The following proteins of this network were increased in abundance: Prohibitin; Albumin; Tumor metastatic process-associated protein NM23; and Glutathione peroxidase. In summary, 5 proteins that increased in abundance with developmental CSE were attributed to redundant membership in these two metabolic networks.

Figure 7 shows the *lipid metabolism, small molecule biochemistry, and carbohydrate metabolism network*. The proteins shaded gray in this figure had *increased* abundance in the kidney of the CSE group. The Solute Carrier Family 2 (Facilitated Glucose Transporter Member 4) protein is again a central node of this network that may be impacted in the kidney by developmental CSE. Increased pixel density of three spots on the 2D gels consisting of four additional proteins in the kidney lipid metabolism, small molecule biochemistry, and carbohydrate metabolism networks connected to the SLC2A4 node further supports the impact of developmental CSE on kidney metabolic networks.

4. DISCUSSION

Cigarette smoke exposure impairs the function of the respiratory, digestive, urogenital, endocrine and cardiovascular systems (Doll, 1996; Hoffman and Hoffman, 1997; Nordlund *et al.*, 1997). In adults, CSE induces kidney glomerular and proximal tubular damage, mesangial cell proliferation in the renal capsule, dilation and congestion in the peritubular capillaries, degeneration in the proximal tubules, and atrophy of the renal capsule (Chu *et al.*, 2001; EL-safty *et al.*, 2003; Czekaj *et al.*, 2002; Odoni *et al.*, 2002). Developmental CSE reduces the proximal tubule cuboidal epithelium thickness, alters the shape of the proximal and distal convoluted tubules, and yields immature glomeruli in neonates (Czekaj *et al.*, 2002; Nelson *et al.*, 1999).

The current study is considered an "active" cigarette smoke exposure model. Maternal cotinine levels, which are indicative of nicotine dosage were above 50 ng/mL. Pup cotinine levels were also increased to a comparable range indicative of "active" cigarette smoke exposure. This "active" CSE during pre- and post-natal development - spanning the entirety of kidney organogenesis - (Kuure *et al.,* 2000; Ingelfinger, 2003) resulted in decreased offspring birthweight and persistent reduced weights throughout postnatal development (13.2% decrease at PD21). Together with our prior finding of decreased crown-rump length, offspring weight, and brain wet weight (Esposito *et al.*, 2008), the reduction in kidney weight in the CSE offspring is interpreted as a proportional decrease in tissue size when normalized to offspring weight.

CSE induced low birth weight is linked to hypertension and diet induced obesity (Doherty *et al.*, 2009; Ng *et al.*, 2009; Oken *et al.*, 2008; Gao *et al.*, 2005) consistent with the Barker hypothesis (Calkins and Devaskar, 2011; Barker *et al.*, 2009; Barker, 1992) which states that an adverse fetal environment results in low birth weight and an increased risk of maturity onset disease. The Brenner hypothesis (Brenner and Chertow; 1994) further postulates a causal association of low birth weight and hypertension. This may in part be attributed to decreased nephron number related to proportionally smaller kidney mass that results in glomerular enlargement and hyperfiltration status once mature organism weight is attained (Benz and Amman, 2010). Of note, a companion study of the liver proteome profiles of CSE offspring notes decreased expression of proteins impacted by retinoic acid availability. A mild reduction in retinoic acid availability during development has been shown to decrease nephron number (Leliever-Pegorier and Merlet-Benichou, 1998). Though nephron number was not assessed, the reduced kidney mass observed in the current study has previously been established as indicative of a reduction in nephron number (Luyckx and Brenner 2010; Xu and Zuo, 2010; Murawski *et al.*, 2010).

Calcium signaling is essential for the conversion of the metanephric mesenchyme into a functional nephron epithelium (Gilbert *et al.*, 2011) with the non-canonical calcium/NFAT Wnt pathway controlling tubulogenesis (Tanigawa *et al.*, 2011; Burn *et al.*, 2011). Calbindin 28K (Spot 18) and Calreticulin (also known as Calregulin; Spot 17) levels were identified as important in the separation of the CSE and Sham groups in the multivariate PLS-DA model with a general trend toward decreased abundance in the kidney of the CSE offspring. Calbindin 28K, a vitamin D dependent calcium binding protein, is present in the mouse metanephric duct from embryonic day 12 and in the advancing ampullae of the ureteric buds (Liu *et al.*, 1993). In the adult, Calbindin 28K is located in the distal convoluted tubule, the connecting tubule, and in the cortical collecting duct (Roth *et al.*, 1981). The CSE-induced decrease in kidney calcium regulatory protein abundance, which indicates a decreased number of tubule segments, is consistent with a decrease in total nephron population.

Similarly in the CSE offspring, kidney antioxidant and chaperone protein expression were altered. Spots identified as Cu/Zn Superoxide Dismutase (Spot 28; increased), Glutathione Peroxidase (Spot 42; increased), Proteasome subunit alpha type 6 (Spot 26; increased), αB-crystallin (Spot 44; increased) and Peroxiredoxin (Spot 11 decreased; also present in Spot 27 and 29 but unable to attribute increased intensity solely to this protein) were found to be important in the separation of the groups by PLS-DA. This finding likely reflects a cellular adaptive response to ongoing cigarette smoke induced oxidative stress which necessitates a scavenging of free radicals and a stabilization of protein secondary and tertiary structures. Of particular interest is the impact of CSE on kidney αB-crystallin, a small heat shock protein with structural and sequence similarity to HSP27. Though crystallins are primarily found in the ocular lens, αB-crystallin is present in extra-ocular tissues and is classified as an inducible small molecular weight chaperone. In the kidney, αB-crystallin expression increases following osmotic stress as well as with oxidative stress (Michl *et al.*, 2006; Beck *et al.*, 2000; Gabert and Kultz, 2011). The observed increase in stress response proteins yields a cellular phenotype that might be incapable of further responding to a secondary stress such as high fat diet. Additional studies are needed to answer whether the kidney from CSE offspring are capable of responding to the hypertonicity accompanying the induction of hypertension.

Glycolysis is a partially reversible central pathway for the catabolism of carbohydrates. In this study, two enzymes shared between the glycolytic/gluconeogenic pathways were decreased in availability: Enolase 1 and Aldolase B. Glyceraldehyde-3-phosphate dehydrogenase and Phosphoglycerate kinase 1 are glycolytic enzymes that do not participate in gluconeogenesis. The decreased abundance of these enzymes supports the interpretation of a probable decrease in glycolytic activity in the kidney of CSE offspring. A corresponding increase in protein abundance related to pyruvate metabolism may reflect a cellular requirement for additional substrate in support of gluconeogenesis or the Tricarboxylic Acid (TCA) cycle. Lactate dehydrogenase B (LDHB) and Mercaptopyruvate sulfurtransferase (MPST) generate pyruvate; Pyruvate dehydrogenase (PDBH) converts pyruvate to acetyl-CoA. However, Malate dehydrogenase, an enzyme in the TCA cycle, was decreased in abundance in the kidney of CSE offspring. Together these data support the interpretation that developmental CSE results in stimulation of gluconeogenesis coupled to limited glycolysis resulting in a deficit in energy production during of kidney development and maturation.

Ingenuity Pathway Analysis was utilized to predict kidney metabolic pathways impacted by developmental CSE. The present study found both *decreased* and *increased* abundance of proteins present as part of the lipid metabolism, small molecule biochemistry and cell cycle network with Solute Carrier Family 2 (SLC2A4; also known as Insulin Dependent Glucose Transporter Member 4, GLUT4) as a central node. SLC2A4 mediates the homeostatic transport of glucose from the blood into cell cytoplasm (Mueckler *et al.*, 1994). Insulin, which mediates cellular uptake of glucose from the blood, was identified as a node of interest as well in *both* the inflammatory disease, respiratory disease and nucleic acid metabolism pathway *and* the lipid metabolism, small molecule biochemistry, and carbohydrate metabolism network. These findings also point to a deficit in cellular kidney glucose availability accompanying developmental CSE.

In summary, the current study examined proteome profiles from whole kidney homogenates and thus cannot directly shed light on glomerular or tubule dysfunction though the finding of smaller kidney mass indicates decreased nephron number. Developmental cigarette smoke exposure alters several metabolic networks in the kidney including the lipid metabolism, small molecule biochemistry, carbohydrate metabolism network *and* the inflammatory disease, respiratory disease and nucleic acid metabolism networks. In contrast to the finding

of impaired gluconeogenesis in the liver of these offspring, a stimulation of kidney gluconeogenic activity was noted and may reflect a systemic lack of glucose availability. We interpret the findings of this study as an indication that continuing CSE on the background of low birth weight (LBW) leads to systemic metabolic dysregulation characterized by impaired chaperoning/antioxidant scavenging and lipid dysregulation as well as impaired glucose metabolism. The impact of CSE cannot be separated from LBW in the current model though the coupled decrease in nephron number may compromise kidney function post-cessation of exposure in adulthood or in the presence of a subsequent challenge. Whether these metabolic alterations in the kidney persist past the cessation of exposure and into maturity is the subject of future studies.

Acknowledgments

References

Abitbol CL, Ingelfinger JR. Nephron mass and cardiovascular and renal disease risks. Semin Nephrol. 2009; 29(4):445–54. [PubMed: 19615565]

Barker DJ. Fetal growth and adult disease. Br J Obstet Gynaecol. 1992; 99:275–6. [PubMed: 1581269]

Barker DJ, Osmond C, Kajantie E, Eriksson JG. Growth and chronic disease: findings in the Helsinki Birth Cohort. Ann Hum Biol. 2009; 36:445–58. [PubMed: 19562567]

Beck FX, Grünbein R, Lugmayr K, Neuhofer W. Heat shock proteins and the cellular response to osmotic stress. Cell Physiol Biochem. 2000; 10:303–6. [PubMed: 11125209]

Benz K, Amman K. Maternal nutrition, low nephron number and arterial hypertension in later life. Biochim Biophys Acta. 2010; 1802(12):1309–17. [PubMed: 20226855]

Boadi WY, Urbach J, Barnea ER, Brandes JM, Yannai S. Enzyme activities in the term human placenta: In vitro effect of cadmium. Pharmacology and Toxicology. 1992; 71:209–212. [PubMed: 1438044]

Bradford M. Analytical Biochemistry. 1976; 72:248. [PubMed: 942051]

Brenner BM, Chertow GM. Congenital oligonephropathy and the etiology of adult hypertension and progressive renal injury. Am J Kidney Dis. 1994; 23:171–5. [PubMed: 8311070]

Burn SF, Webb A, Berry RL, Davies JA, Ferrer-Vaquer A, Hadjantonakis AK, Hastie ND, Hohenstein P. Calcium/NFAT signalling promotes early nephrogenesis. Dev Biol. 2011; 352:288–98. [PubMed: 21295565]

Calkins K, Devaskar SU. Fetal origins of adult disease. Curr Probl Pediatr Adolesc Health Care. 2011; 41:158–76. [PubMed: 21684471]

Centers for Disease Control and Prevention. Surgeon General's Report. U.S. Department of Health and Human Services Coordinating Center for Health Promotion National Center for Chronic Disease Prevention and Health Promotion Office of Smoking and Health; 2001. Women and smoking.

Centers for Disease Control and Prevention. Low Birth Weight and Growth Retardation in the Environment. 2010. Reproduction and Birth Outcomes.

Chu P, Lu K, Lin Y. Acute correction of metabolic acidosis increases serum procollagen type I carboxyterminal propeptide in patients with chronic renal failure. J Formos Med Assoc. 2001; 100:748–52. [PubMed: 11802533]

Czekaj P, Pałasz A, Lebda-Wyborny T, Nowaczyk-Dura G, Karczewska W, Florek E, Kami ski M. Morphological changes in lungs, placenta, liver and kidneys of pregnant rats exposed to cigarette smoke. Int Arch Occup Environ Health. 2002; 75:S27–S35. [PubMed: 12397408]

Doherty SP, Grabowski J, Hoffman C, Ng SP, Zelikoff JT. Early life insult from cigarette smoke may be predictive of chronic diseases later in life. Biomarkers Suppl. 2009; 1:97–101.

Doll R. Cancers weakly related to smoking. British Medical Bulletin. 1996; 52:35–49. [PubMed: 8746295]

El-Safty IA, Gadallah M, Shouman AE, Nessim DE. Subclinical nephrotoxicity caused by smoking and occupational silica exposure among Egyptian industrial workers. Arch Med Res. 2003; 34:415–421. [PubMed: 14602509]

Esposito ER, Horn KH, Greene RM, Pisano MM. An animal model of cigarette smoke-induced in utero growth retardation. Toxicology. 2008; 246:193–202. [PubMed: 18316152]

Gabert BJ, Kültz D. Osmoprotective proteome adjustments in mouse kidney papilla. Biochim Biophys Acta. 2011; 1814:435–48. [PubMed: 21236367]

Gao Y, Holloway JA, Zeng CZ, Lim HG, Petrik EJJ, Foster WG, Lee RM. Prenatal exposure to nicotine causes postnatal obesity and altered perivascular adipose tissue function. Obes Res. 2005; 13:687–92. [PubMed: 15897477]

Gilbert T, Leclerc C, Moreau M. Control of kidney development by calcium ions. Biochimie. 2011 [Epub ahead of print].

Hoffman D, Hoffman I. The changing cigarette, 1950–1995. J Toxicol Environ Health. 1997; 50:307–364. [PubMed: 9120872]

Hughson M, Farris AB, Douglas-Denton R, Hoy WE, Bertram JF. Glomerular number and glomerular size in autopsy kidneys: the relationship to birth weight. Kidney Int. 2003; 63:2113–2122. [PubMed: 12753298]

Ingelfinger JR. Congenital ureteral obstruction: new technology, new targets. Kidney Int. 2003; 64:25–35. [PubMed: 12787392]

Ingenuity Systems. [Accessed on October 27, 2010] Ingenuity Pathway Analysis: Overview. http://www.ingenuity.com/products/pathways_analysis.html

Karp NA, Griffin JL, Lilley KS. Application of partial least squares discriminant analysis to two-dimensional difference gel studies in expression proteomics. Proteomics. 2005; 5:81–90. [PubMed: 15744836]

Kuure S, Vuolteenaho R, Vainio S. Kidney morphogenesis: cellular and molecular regulation. Mechanisms of development. 2000; 92:31–45. [PubMed: 10704886]

Kyerematen GA, Vesell ES. Metabolism of Nicotine. Drug metabolic review. 1991; 23:3–41.

Lelievre-Pegorier M, Vilar J, Ferrier ML, Moreau E, Freund N, Gilbert T, Merlet-Benichou C. Mild vitamin A deficiency leads to inborn nephron deficit in the rat. Kidney Int. 1998; 54(5):1455–1462. [PubMed: 9844121]

Liu L, Dunn ST, Christakos S, Hanson-Painton O, Bourdeau JE. Calbindin-D28k gene expression in the developing mouse kidney. Kidney Int. 1993; 44:322–30. [PubMed: 8377376]

Luyckx VA, Brenner BM. The clinical importance of nephron mass. J Am Soc Nephrol. 2010; 21:898–910. [PubMed: 20150537]

Smoking During Pregnancy. Apr. 2010 March of Dimes. Retrieved on May 12, 2010

Michl M, Ouyang N, Fraek ML, Beck FX, Neuhofer W. Expression and regulation of alphaB-crystallin in the kidney in vivo and in vitro. Pflugers Arch. 2006; 452:387–95. [PubMed: 16680485]

Mueckler M. Facilitated Glucose Transporters. Eur J Biochem. 1994; 219:713–725. [PubMed: 8112322]

Murawski IJ, Maina RW, Gupta IR. The relationship between nephron number, kidney size and body weight in two inbred mouse strains. Organogenesis. 2010; 6:189–94. [PubMed: 21197222]

Nelson E, Goubet-Wiemers C, Guo Y, Jodscheit K. Maternal passive smoking during pregnancy and foetal developmental toxicity. Part 2: histological changes. Hum Exp Toxicol. 1999; 18:257–64. [PubMed: 10333312]

Neuhoff V, Stamm R, Eibl H. Clear background and highly sensitive protein staining with Coomassie Blue dyes in polyacrylamide gels: a systematic analysis. Electrophoresis. 1985; 6:427–448.

Ng SP, Conklin DJ, Bhatnagar A, Bolanowski DD, Lyon J, Zelikoff JT. Prenatal exposure to cigarette smoke induces diet- and sex-dependent dyslipidemia and weight gain in adult murine offspring. Environ Health Perspect. 2009; 117:1042–8. [PubMed: 19654910]

Nordlund LA, Carstensen JM, Pershagen G. Cancer incidence in female smokers: A 26 year follow up. Int J Cancer. 1997; 73:625–628. [PubMed: 9398036]

Odoni G, Ogata H, Viedt C, Amann K, Ritz E, Orth SR. Cigarette smoke condensate aggravates renal injury in the renal ablation model. Kidney International. 2002; 61:2090–8. [PubMed: 12028449]

Oken E, Levitan EB, Gillman MW. Maternal smoking during pregnancy and child overweight: systematic review and meta-analysis. Int J Obes (Lond). 2008; 32:201–10. [PubMed: 18278059]

Rahman I, Nee Mac. Oxidant/antioxidant imbalance in smokers and chronic obstructive pulmonary disease. Thorax. 1996; 51:348–350. [PubMed: 8733482]

Roth J, Thorens B, Hunziker W, Norman AW, Orci L. Vitamin D--dependent calcium binding protein: immunocytochemical localization in chick kidney. Science. 1981; 214:197–200. [PubMed: 7025212]

Society for Research on Nicotine, Tobacco Subcommittee on Biochemical Verification . Biochemical verification of tobacco use and cessation. Nicotine Tob Res. 2002; 4(2):149–59. [PubMed: 12028847]

Shah PK, Helfant RH. Smoking and coronary artery disease. Chest. 1988; 94:449–452. [PubMed: 3409719]

Shea AK, Steiner M. Cigarette smoking during pregnancy. Nicotine and Tobacco research. 2008; 10:267–278. [PubMed: 18236291]

Sisman AR, Bulbul M, Coker C, Onvural B. Cadmium exposure in tobacco workers: possible renal effects. Journal of trace elements and Medical Biology. 2003; 17:51–55.

Substance Abuse and Mental Health Services Administration. Office of Applied Studies. National Household Survey on Drug Abuse; 1999.

Stack AG, Murthy AV. Cigarette use and cardiovascular risk in chronic kidney disease: An unappreciated modifiable lifestyle risk factor. Seminars in Dialysis. 2010; 23:298–305. [PubMed: 20636923]

Tanigawa S, Wang H, Yang Y, Sharma N, Tarasova N, Ajima R, Yamaguchi TP, Rodriguez LG, Perantoni AO. Wnt4 induces nephronic tubules in metanephric mesenchyme by a non-canonical mechanism. Dev Biol. 2011; 352:58–69. [PubMed: 21256838]

Teague, SV.; Pinkerton, KE.; Goldsmith, M.; Gebremichael, A.; Chang, S. Sidestream cigarette smoke generation and exposure system for environmental tobacco smoke studies. 1994.

Tomatis, L. Overview of perinatal and multigeneration carcinogenesis. In: Napapkov, NP.; Rice, JM.; Tomatis, L.; Yamasaki, H., editors. Prenatal and Multigeneration Carcinogenesis. Agency for Research on Cancer; Lyon France: 1989. p. 1-15.Sci. Publ., No.96

Xu R, Zuo L. Low birthweight and chronic kidney disease. Nephrology (Carlton). 2010; 15(Suppl 2): 18–22. [PubMed: 20586942]

Zavos PM. Cigarette smoking and human reproduction: effects on female and male fecundity. Infertility. 1989; 12:35–46.

Zdravkovic T, Genbacev O, McMaster MT, Fisher SJ. The adverse effects of maternal smoking on the human placenta: a review. Placenta. 2005; 26:S81–S86. [PubMed: 15837073]
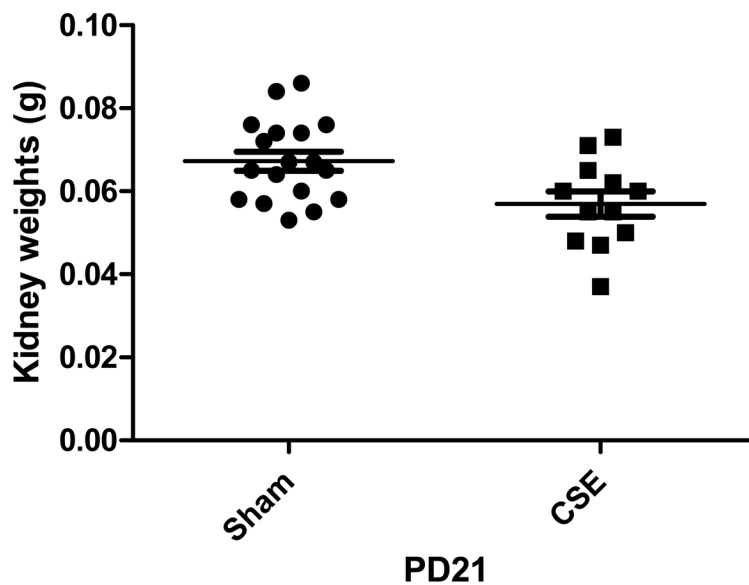
Figure 1. Offspring Kidney Mass is Decreased by Developmental CSE
Pup kidneys of C57Bl/6 mice exposed to CSE (cotinine >50 ng/mL) from GD1-PD21 were decreased in mass as compared to the kidneys of Sham (filtered air) exposed C57Bl/6 mice (p<0.01). The observed ~15% decrease in kidney mass is proportional to the reduction in birth weight and persistent decreased weight of these offspring.
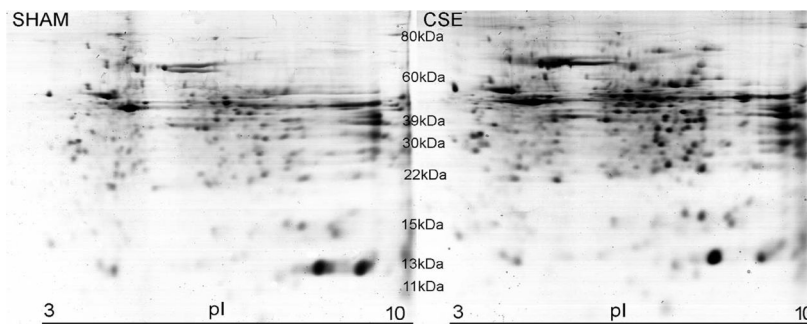
**Figure 2. Representative 2D-SDS-PAGE Gel: Protein Spot Profiles of the Kidneys from Sham and CSE Offspring**
A side-by-side comparison of kidney protein spot separation based on isoelectric focusing point (horizontal) and molecular weight (vertical) in the two experimental groups (Sham-left; CSE-right). The gels are similar in number of spots without the appearance or loss of spots between experimental groups.

Figure 3A:

Latent Factor	Y Variance	Cumulative Y Variance (R squared)
1	.58	.58
2	.32	.90
3	.07	.97

Figure 3B:
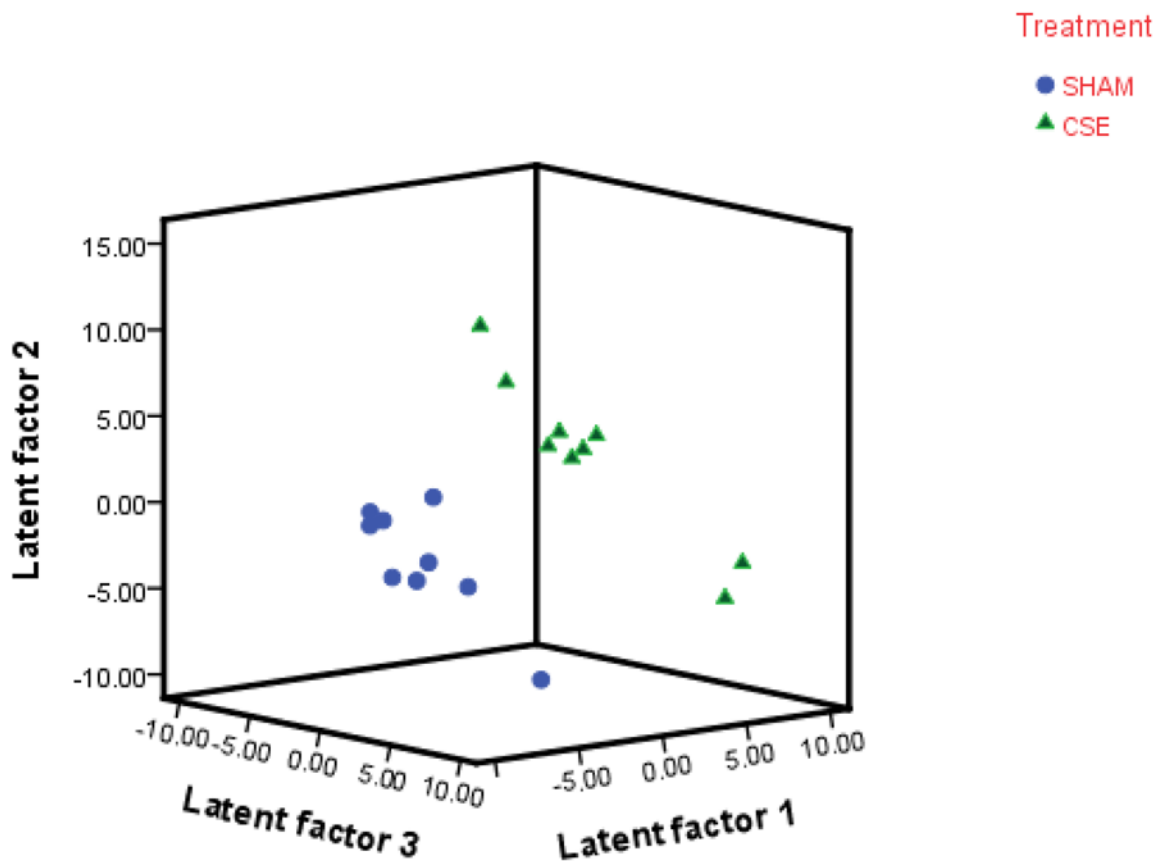
Figure 3.

Figure 3A: Variable Importance in Projection. Protein spots present on gels from the Sham exposed and CSE groups were analyzed by PLS-DA (n=9 per group, biological replicates). Description of the separation of groups by latent factors found that 97% of the variance between groups could be described by three latent factors.

Figure 3B: Plotting Latent Factors from the PLS-DA model shows differences in the kidney protein spot patterns of the Sham exposed and CSE groups. All protein spots (excluding noise) were included in the calculation of VIP rankings and the graphing of the separation of groups by latent factors.
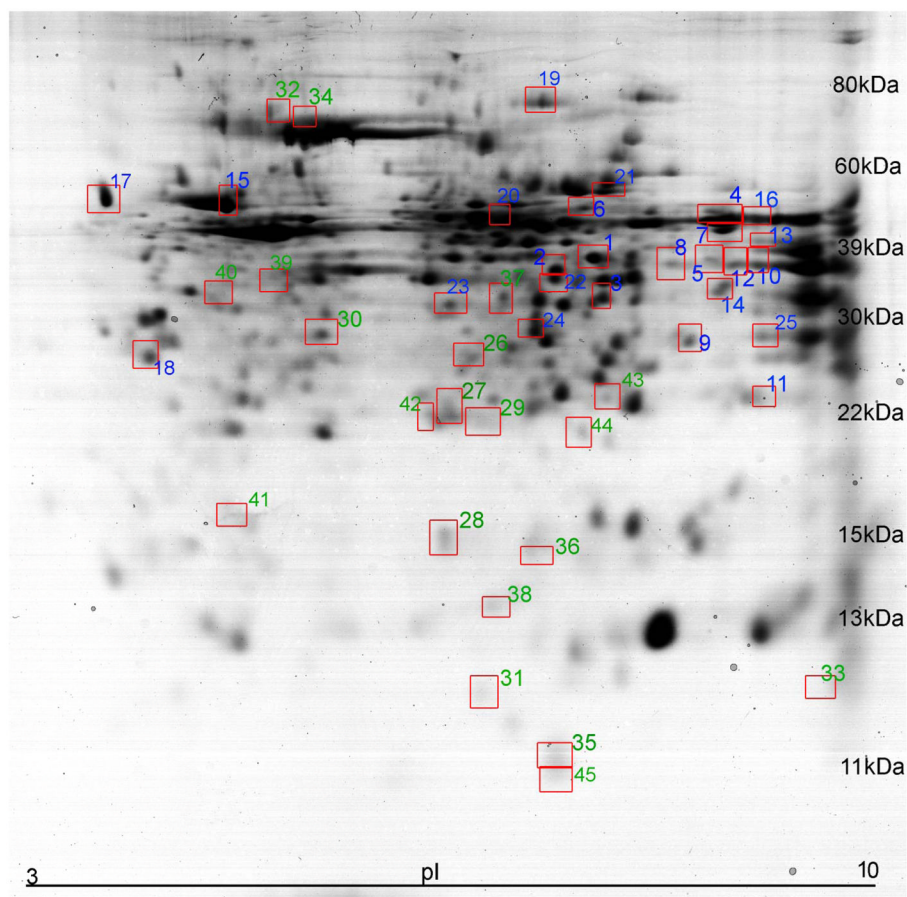
Figure 4. Differential Abundance of Kidney Proteins
Protein spots with altered pixel density in the kidneys of the CSE group are outlined and numbered. Green indicates *increased* spot pixel density and blue indicates *decreased* spot pixel density in the CSE group. Refer to Table 1 for a listing of proteins identified in each spot.
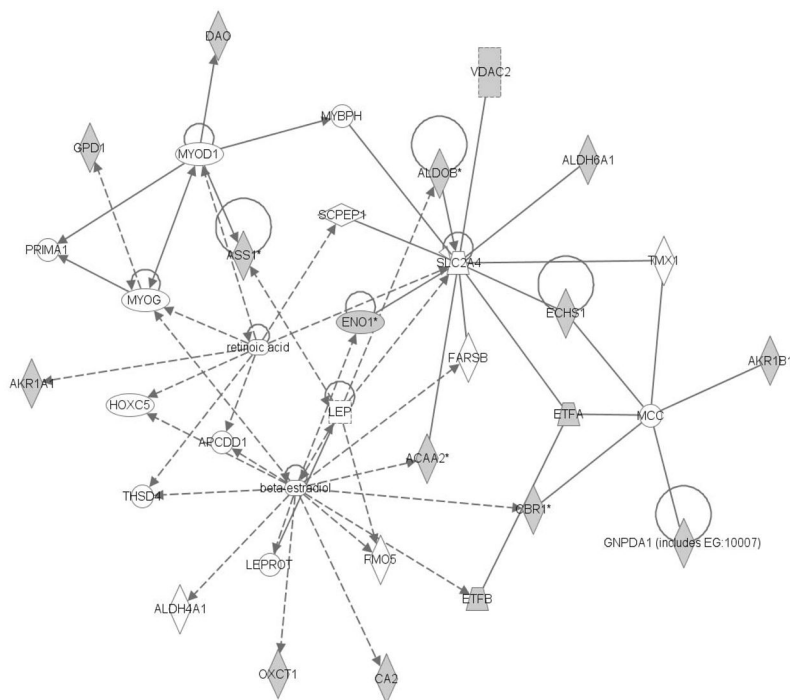
Figure 5. The Lipid Metabolism and Small Molecule Biochemistry Network of the Kidney is Impacted by Developmental CSE
Kidney proteins identified as contributing to the separation of groups (Sham exposed and CSE) are shadowed and connected to the network by arrows denoting directionality of impact. All shadowed proteins were *decreased* in abundance.
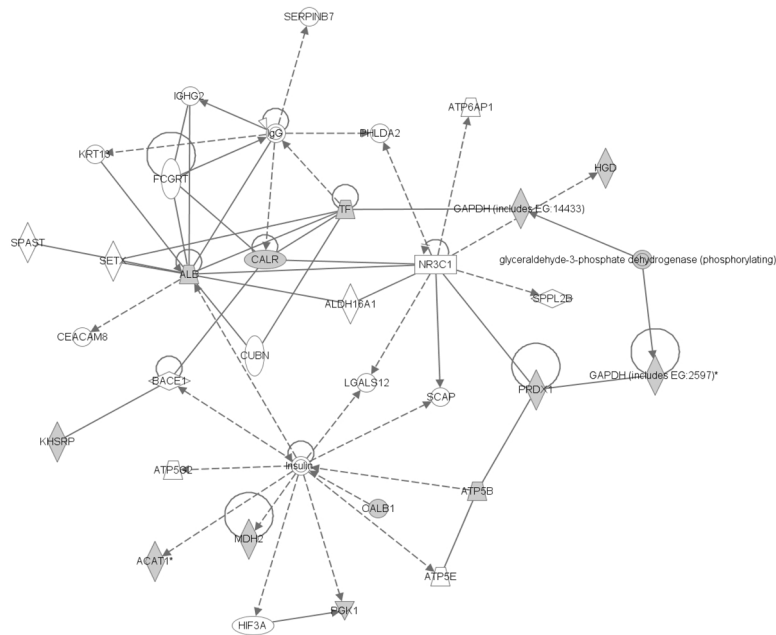
Figure 6. The Inflammatory Disease, Respiratory Disease and Nucleic Acid Metabolism Network of the Kidney is Impacted by Developmental CSE
Proteins identified as contributing to the separation of groups by PLS-DA (Sham exposed and CSE) are shadowed and connected to the network by arrows denoting directionality of impact. All shadowed proteins were present in protein spots with *decreased* abundance.
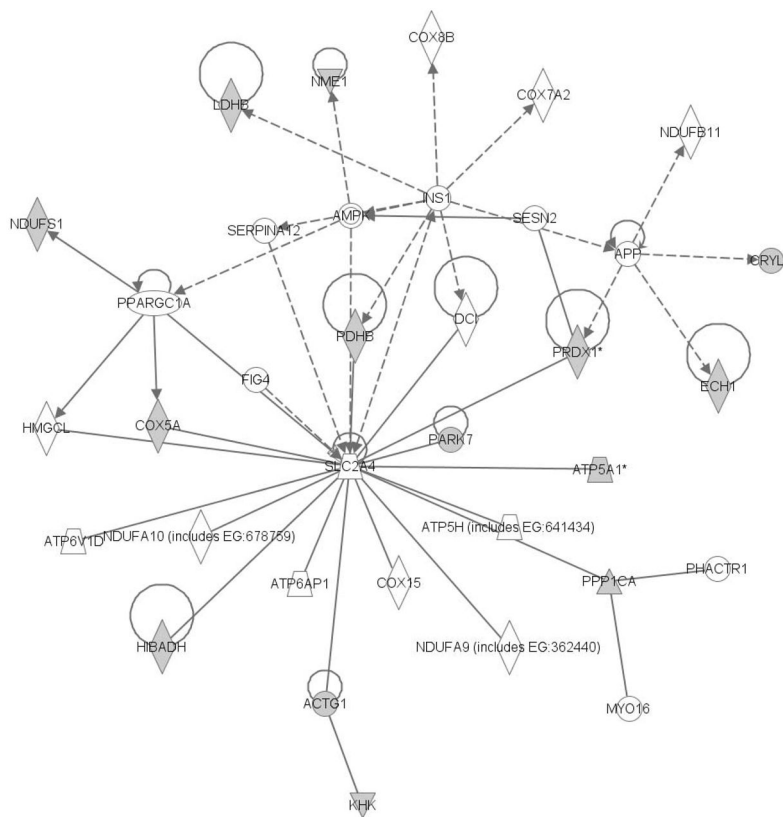
Figure 7. The Lipid Metabolism, Small Molecule Biochemistry, and Carbohydrate Metabolism Network of the Kidney is Impacted by Developmental CSE
Proteins identified as contributing to the separation of groups by PLS-DA (Sham exposed and CSE) are shadowed and connected to the network by arrows denoting directionality of impact. All shadowed proteins were present in protein spots with *increased* abundance.

Table 1

Identification of Proteins in Spots with Decreased and Increased Pixel Density that Contributed to the Separation of Sham and CSE groups (PLS-DA model)

Data corresponds to Figure 4 (numbers in blue represent spots with apparent decreased pixel density and numbers in green represents spots with apparent increased pixel density).

Spot	ANOVA	VIP	Name	Score	Abb. Name
1	0.001	3.46	Aldo-keto reductase family 1, member A4 (aldehyde reductase), gi|10946870	671	AKR1A1
			D-amino acid oxidase, gi|198572	138	DAO
2	0.002	3.32	Aldose reductase, gi|3046247	477	AKR1B1
3	0.019	2.67	Voltage-dependent anion channel 2, gi|6755965	515	VDAC2
			Electron transferring flavoprotein, alpha polypeptide, gi|13097375	384	ETFA
4	0.042	2.61	Phosphoglycerate kinase, gi|202423	688	PGK1
			Argininosuccinate synthetase 1, gi|6996911	672	ASS1
			Acetyl-Coenzyme A acyltransferase 2 (mitochondrial 3-oxoacyl-Coenzyme A thiolase), gi|29126205	480	ACAA2
			Acetyl-Coenzyme A acetyltransferase 1 precursor, gi|21450129	201	ACAA1
5	0.036	2.45	PREDICTED: similar to glyceraldehyde-3-phosphate dehydrogenase, gi|62653546	432	GAPDH
6	0.067	2.34	Homogentisate 1, 2-dioxygenase, gi|37572245	349	HGD
			Hypothetical protein LOC433182, gi|55491	279	-
			2-phosphopyruvate-hydratase alpha-enolase, gi|693933	269	ENO1
7	0.063	2.34	Acetyl-Coenzyme A acetyltransferase 1 precursor, gi|21450129	555	ACAA1
8	0.051	2.27	PREDICTED: similar to glyceraldehyde-3-phosphate dehydrogenase, gi|62653546	449	GAPDH
9	0.057	2.14	Mitochondrial short-chain enoyl-coenzyme A hydratase 1, gi|12805413	538	ECHS1
10	0.057	2.13	PREDICTED: similar to glyceraldehyde-3-phosphate dehydrogenase, gi|62653546	432	GAPDH
11	0.143	2.10	Peroxiredoxin 1, gi|6754976	460	PRDX1
			rCG64140, gi|149025344	136	
12	0.140	2.04	Glyceraldehyde-3-phosphate dehydrogenase, gi|6679937	486	GAPDH
13	0.095	2.02	Aldolase B, fructose-bisphosphate, gi|21450291	476	ALDOB
			Similar to glyceraldehyde-3-phosphate dehydrogenase, gi|62653546	270	GAPDH
14	0.094	2.00	Malate dehydrogenase 2, NAD (mitochondrial), gi|31982186	636	MDH2
			Carbonyl reductase 1, gi|113680352	402	CBR1

Spot	ANOVA	VIP	Name	Score	Abb. Name
			Inducible carbonyl reductase, gi|1906812	192	CBR1
15	0.080	1.93	Mitochondrial ATP synthase beta subunit, gi|31980648	1121	ATP5B
16	0.091	1.65	Acetyl-Coenzyme A acyltransferase 2 (mitochondrial 3-oxoacyl-Coenzyme A thiolase), gi|29126205	486	ACAA2
			Argininosuccinate synthetase 1, gi|6996911	427	ASS1
17	0.146	1.98	Calreticulin, gi|6680836	314	CALR
18	0.217	1.70	Calbindin-28K, gi|6753242	356	CALB1
19	0.110	1.99	Transferrin, gi|17046471	1340	TF
			KH-type splicing regulatory protein, gi|9424312	235	KHSRP
			Albumin,gi|158138568	165	ALB
20	0.238	1.60	Eno1 protein, gi|34784434	311	ENO1
			Hypothetical protein LOC433182, gi|70794816	310	-
21	0.153	1.82	3-oxoacid CoA transferase 1, gi|189181716	259	OXCT1
			Methylmalonate-semialdehyde dehydrogenase (Aldehyde dehydrogenase family 6 member A1), gi|400269	226	ALDH6A1
22	0.206	1.65	Glycerol-3-phosphate dehydrogenase, gi|387177	404	GPD1
23	0.300	1.51	Citrate lyase beta like, gi|19173728	356	-
			Glucosamine-6-phosphate isomerase 1, gi|12644084	257	GNPDA1
24	0.162	1.85	Carbonic anhydrase II, gi|157951596	252	CA2
			Fructose-bisphosphate aldolase B, gi|15723268	144	ALDOB
25	0.261	1.60	Electron transferring flavoprotein, beta polypeptide, gi|38142460	514	ETFB
			3-hydroxybutyrate dehydrogenase, type 2, gi|23956202	168	BDH2
26	0.015	2.70	Proteasome (prosome, macropain) subunit, alpha type 6, gi|6755198	230	PSMA6
27	0.024	2.71	ATP synthase, H+ transporting, mitochondrial F1 complex, alpha subunit, isoform 1, gi|127798841	558	ATP5B
			Glutathione peroxidase, gi|2673845	317	GPX1
			Peroxiredoxin 1, gi|6754976	252	PRDX1
28	0.031	2.58	Cu/Zn superoxide dismutase, gi|226471	276	SOD
29	0.058	2.22	ATP synthase, H+ transporting, mitochondrial F1 complex, alpha subunit, isoform 1, gi|6680748	303	ATP5A1
			Peroxiredoxin 1, gi|6754976	221	PRDX1
30	0.070	2.03	Prohibitin, gi|6679299	623	PHB
			Gamma-actin, gi|809561	185	ACTG1

Spot	ANOVA	VIP	Name	Score	Abb. Name
31	0.070	2.26	Not identified		-
32	0.081	2.24	NADH-ubiquinone oxidoreductase 75 kDa subunit, gi|47117271	922	NDUFS1
33	0.085	1.86	Trypsin, gi|136429	129	-
34	0.087	1.73	Albumin, gi|163310765	211	ALB
35	0.163	2.14	mCG13235, gi|148684097	159	-
			PREDICTED: similar to polyubiquitin, gi|109497721	152	-
36	0.088	2.08	Tumor metastatic process-associated protein NM23, gi|387496	211	NME1
37	0.116	2.01	Enoyl coenzyme A hydratase 1, peroxisomal, gi|7949037	431	ECH1
			Carbonyl reductase 3, gi|27413160	337	CBR3
			3-hydroxyisobutyrate dehydrogenase precursor, gi|21704140	282	HIBADH
			Mercaptopyruvate sulfurtransferase, gi|63100260	275	MPST
			Ketohexokinase/Hepatic fructokinase, gi|6016435	128	KHK
38	0.101	1.86	Not identified		-
39	0.126	1.85	L-lactate dehydrogenase B, gi|6678674	595	LDHB
			Albumin, gi|163310765	303	ALB
			Crystallin, lambda 1, gi|19525729	300	CRYL1
			Pyruvate dehydrogenase (lipoamide) beta, gi|18152793	278	PDHB
			Capping protein alpha 1 subunit, gi|595917	223	CAPZA1
			Copper binding protein/S-adenosyl-L-homocysteine hydrolase, gi|904132	217	AHCY
			Protein phosphatase 1, catalytic subunit, alpha, gi|13994195	196	PPP1CA
			Potassium channel tetramerization domain containing 12, gi|123701966	170	KCTD12
40	0.176	1.66	Elongation factor 1-delta, gi|13124192	139	EEF1D
			Epsilon subunit of coatomer protein complex, gi|10946972	132	COPE
41	0.135	1.69	Cytochrome c oxidase subunit Va preprotein, gi|50527	110	COX5A
42	0.126	1.74	Glutathione peroxidase, gi|2673845	400	GPX1
			Parkinson disease protein 7, gi|55741460	191	PARK7
43	0.112	1.58	Not identified		-
44	0.229	1.54	Crystallin, alpha B, gi|6753530	201	CRYAB
45	0.251	1.51	PREDICTED: similar to polyubiquitin, gi|109497721	144	-